Biophysical Chemistry, 47 (1993) 33–40
Elsevier Science Publishers B.V., Amsterdam

BIOCHE 01756

Intensity and anisotropy decays of [Leu^5] enkephalin tyrosyl fluorescence by 10 GHz frequency-domain fluorometry

Joseph R. Lakowicz *, Ignacy Gryczynski, Gabor Laczko and Wieslaw Wiczk

University of Maryland School of Medicine, Center for Fluorescence Spectroscopy, Department of Biological Chemistry, 108 North Greene Street, Baltimore, MD 21201 (USA)

(Received 3 December 1990; accepted in revised form 22 January 1993)

Abstract

The technique of 10 GHz frequency-domain fluorometry was used to resolve the complex picosecond intensity and anisotropy decays of the tyrosyl emission of [Leu^5] enkephalin. Enhanced resolution of anisotropy decay was obtained by using acrylamide quenching of the tyrosyl fluorescence and global analysis of the frequency-domain anisotropy data obtained with different amounts of acrylamide. The data indicates a 44 ps correlation time for local tyrosine motions, and a 219 ps correlation time for overall rotational diffusion of the pentapeptide. Our data are consistent with an initial loss of fluorescence anisotropy from $r_0 = 0.4$ to a value of $r_0 = 0.326$ occurring during the first two picoseconds after excitation.

Keywords: Frequency-domain fluorometry; Anisotropy decays; Molecular dynamics; Fluorescence spectroscopy; [Leu^5] enkephalin

1. Introduction

Time-resolved fluorescence spectroscopy is a powerful technique for quantifying the dynamics of macromolecules [1,2]. In proteins, the tyrosyl and tryptophyl residuals serve as intrinsic probes. Using their emissions, it has been possible to detect the local dynamic motions of these residues, as well as overall rotational diffusion of the proteins [3–5]. If the time resolution is adequate, then it is of interest to compare the experimental measurements of protein dynamics with the prediction of molecular dynamics calculations [6–8]. However, to date, the time resolution of fluorescence spectroscopy has not been adequate for this task, and has been limited by the pulse widths of light sources and the timing limitations of photomultiplier tubes [9] and associated timing electronics [9,10].

In an attempt to improve the time resolution of the fluorescence measurements, this laboratory [11,12] and others [13] developed the frequency-domain method for the resolution of complex fluorescence intensity [14,15] and anisotropy decays [16,17]. The resolution of rapid and/or complex decays is limited by the upper frequency limit of the measurements. The first frequency-domain measurements with modulation frequencies up to 200 MHz were shown to provide good

* To whom correspondence should be addressed.

resolution of multi-exponential intensity and anisotropy decays [14–17]. Among a multitude of advances in instrumentation and analysis, the extension of the frequency range to 2 GHz [11] and then 10 GHz [12] had the most dramatic effect in improved resolution of rapid and/or complex decay processes [18,19]. Correlation times as short as 7 ps have been measured using the 2 GHz instrument [20], and still shorter correlation times could be measured using our 10 GHz instrument [12].

In this report, we describe the first measurements of protein tyrosyl intensity and anisotropy decays using the 10 GHz frequency-domain instrument [12]. In a previous study, we reported a 1.4 ns decay time and a 0.33 ns correlation time for [Leu^5] enkephalin (Tyr–Gly–Ghy–Phe–Leu), the values being obtained at a single modulation frequency of 30 MHz [21]. In a later study, using the 2 GHz instrument [18], we reported more complex intensity and anisotropy decays for this peptide. Laws and coworkers also found a complex fluorescence intensity decays for several tyrosine analogues and small peptides, which they attributed to the rotamer populations [22,23]. In the present study, we use the 10 GHz measurements to obtain picosecond time resolution of the tyrosyl anisotropy decay of enkephalin.

2. Materials and methods

Frequency-domain data were obtained on the instrument described previously [12]. This instrument is comparable to other frequency-domain fluorometers, except for the following modifications: (1) The sub-GHz frequency synthesizer was replaced by 18 GHz (Gigatronics, Model 905), (2) The microchannel plate (MCP) photomultiplier tube (Hamamatsu R1564) was replaced by triode-type R2566 with 6 μm channels (also Hamamatsu), (3) Electronics (amplifiers, cables, connectors, mixers, etc.) were replaced by higher frequency (18 GHz) devices and, (4) Cross-correlation detection of the high frequency signals is accomplished outside the MCP PMT in microwave mixing circuits [12].

[Leu^5] enkephalin was obtained from Bachem, Inc. and HPLC analysis shown more than 99% purity. Its emission spectrum was characteristic of tyrosine. High purity acrylamide (99.9%) was from BioRad. The experiments were performed in 50 mM Tris (pH 7) at 20°C, using 287 nm excitation (rhodamine 6G dye laser plus frequency doubler). The emission was observed through a 302 nm interference filter (10 nm bandpass). Examination of buffer alone indicated that background fluorescence and/or scattered light contributed less than 0.5% to the measured emission. The anisotropy spectrum was measured in propylene glycol at −60°C.

The intensity decays were analyzed in terms of a sum of exponentials,

$$I(t) = \sum_i \alpha_i \exp[-t/\tau_i] \qquad (1)$$

where α_i are the preexponential factors and τ_i the decay times. The anisotropy decays were also analyzed using a multi-exponential model,

$$r(t) = \sum_j (r_0 g_j) \exp(-t/\theta_j) \qquad (2)$$

where $r_0 g_j$ are the amplitudes associated with each correlation time θ_j. The fundamental anisotropy in the absence of rotational diffusion (r_0) can be considered to be known from other data, or can be considered to be a variable parameter. If r_0 is known, then there are $(j-1)$ variable amplitudes (g_j). If r_0 is not known then these are j variable amplitudes ($r_0 g_j = r_j$). The frequency domain data were analyzed using methods previously described in detail [14–17]. For all analyses the uncertainties in the phase ($\delta\phi$) and modulation (δm) values were taken as 0.2° and 0.005, respectively. These values were found, over a period of years, to be typical of our instrument and methods of measurement.

3. Results

Frequency-domain data for the intensity decay analysis are shown in Fig. 1. The data extend from 20 MHz to 2 GHz for unquenched sample and to 9 GHz when the fluorescence was

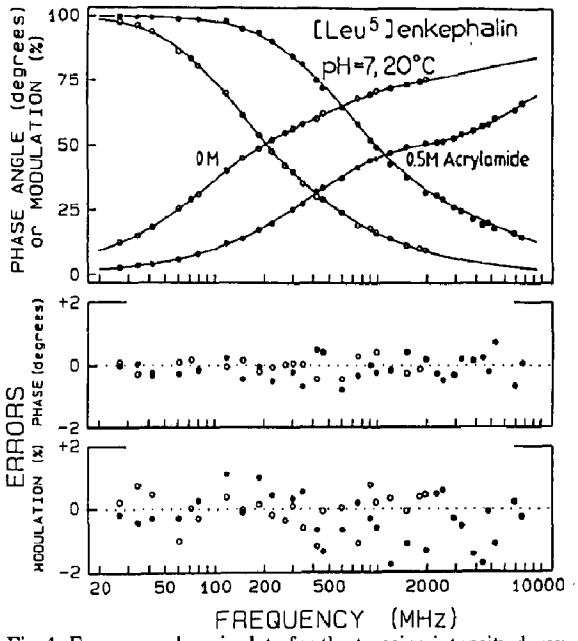

Fig. 1. Frequency-domain data for the tyrosine intensity decay of [Leu^5] enkephalin in absence (○) and presence (●) of 0.5 M acrylamide. The solid lines show the best three decay time fits to the data.

quenched by 0.5 M acrylamide. The 2 GHz limit for the unquenched samples is the result of the long decay time, which results in extensive demodulation of the emission at the higher frequencies. Addition of 0.5 M acrylamide results in a four- to five-fold decrease in the mean decay time from 1.3 ns to 284 ps (Table 1). Then, the frequency-domain data can be measured to 9 GHz. In both the presence and absence of acrylamide, three exponential components are needed to account for the data. The one- and two-component fits are not acceptable, resulting in $\chi^2_R = 655.2$ and 13.5, respectively, for the unquenched sample. The heterogeneity of the intensity decay is increased for the quenched sample, due to transient effects in collisional quenching [24,25]. We note that the decay in the presence of quencher is probably not a true multi-exponential decay, and then the α_i and τ_i values in Table 1 should be regarded as a mathematical description of the intensity decay and not as representing discrete emitting species and/or molecular populations [26]. The Stern–Volmer constant for acrylamide quenching, calculated using mean lifetimes for the unquenched and quenched samples (Table 1) is approximately $K_{sv} = 7.2\ M^{-1}$, which is close to the value obtained for N-acetyltyrosinamide ($K_{sv} = 10\ M^{-1}$ [27]). This shows that the tyrosyl group in [Leu^5] enkephalin is almost fully exposed to the solvent, and the other four amino acids do not shield it from acrylamide quenching. However, we note that the precise value and interpretation of the Stern–Volmer constant is not important for the present analysis because the quenching process is being used to decrease the lifetime of the excited state, and thereby obtain increased information content at early times following excitation.

Collisional quenching of fluorescence is known to be an effective method to increase resolution in complex anisotropy decays [20,28,29]. The emission which is observed under quenching conditions contains an increased proportion of early emitters because quenching selectively removes the longer lived fluorophores. Data obtained without quenching contains information on processes with decay times comparable to the unquenched lifetime. In this case, the unquenched lifetimes is about 1.3 ns, so that the slower process of overall rotational diffusion is the domi-

Table 1

Intensity decay analysis of [Leu^5] enkephalin tyrosyl emission (20°C, pH 7)

[Acrylamide]	n	τ_i (ps)	$\bar{\tau}$ (ps)	α_i	f_i [b]	χ^2_R
0 M	1 [a]	954	1303 [c]	1	1	655.2
	2	200		0.485	0.118	
		1410		0.515	0.882	13.5
	3	52		0.236	0.016	
		335		0.352	0.156	
		1512		0.412	0.828	1.3
0.5 M	1	148	284	1	1	1883.9
	2	33		0.703	0.195	
		326		0.297	0.805	7.2
	3	30		0.672	0.169	
		207		0.186	0.327	
		418		0.142	0.505	3.1

[a] Number of exponential components.
[b] $f_i = \alpha_i\tau_i / \Sigma\alpha_i\tau_i$.
[c] $\bar{\tau} = \Sigma f_i\tau_i$ from the three component fit.

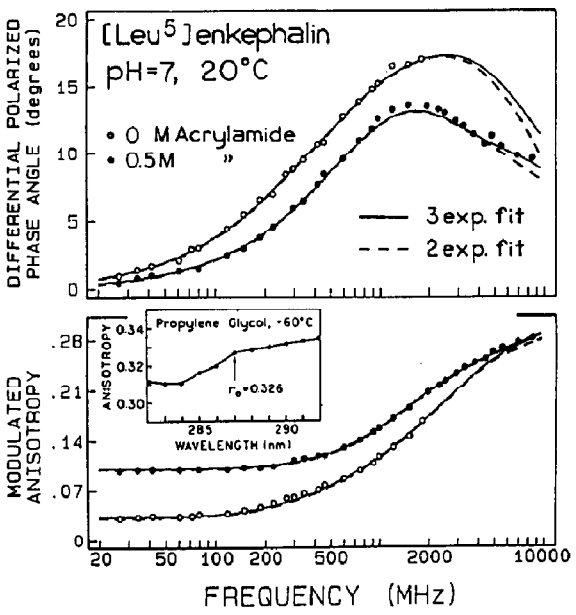

Fig. 2. Frequency-domain data for the tyrosine anisotropy decay of [Leu^5] enkephalin in absence (○) and presence (●) of 0.5 *M* acrylamide. The solid lines show the best global (0 and 0.5 *m* acrylamide) three-exponential fit to the data and the dashed lines show the best global two-exponential fit (with r_0 floating). The insert shows the polarization spectrum of [Leu^5] enkephalin measured in propylene glycol at −60°C using doubled output of a rhodamine 6G dye laser.

nant determinant of the data. Global analysis of the anisotropy data from quenched and unquenched samples provides increased resolution of segmented motions in proteins [28]. This is because these motions dominate the anisotropy decay at short times, and only short decay times are present in the quenched samples.

Frequency-domain data to recover the anisotropy decay kinetics are shown in Fig. 2. These data are the phase angle difference between the polarized components of the emission (top) and the frequency-dependent anisotropy (bottom) [30]. The anisotropy data for the unquenched (open circle) and quenched (solid circle) samples were analyzed simultaneously. The solid lines represent the best two correlation time fit from the global analysis. The differential phase angles in the higher frequency range (above 1 GHz) indicate the presence of motions occurring in tens of picoseconds. Additionally, acrylamide quenching causes an increase in the modulated anisotropy (lower panel). At low modulation frequencies the modulated anisotropy converges towards the steady-state anisotropy [30], which is increased if the decay time is decreased by quenching [31,32]. At higher frequencies the modulated anisotropy depends upon frequency and the rotational rate of the fluorophore, and at frequencies high relative to the rotational rates the modulated anisotropy converges toward r_0.

The anisotropy decay parameters of [Leu^5] enkephalin obtained from single files as well as from global analysis (0 and 0.5 *M* acrylamide) are summarized in Table 2. Attempts to fit the data with a single rotational time resulted in an unacceptable match to the data and in elevation of the χ^2_R value (Table 2). It should be noted that in the one and two correlation time analysis all the correlation times and amplitudes were floating

Table 2

Anisotropy decays of [Leu^5] enkephalin (20°C, pH 7)

[Acrylamide]	n [a]	θ_i (ps)	$r_0 g_i$	χ^2_R
0	1 [a]	120	0.256	15.2
	2	51 (5) [b]	0.237	
		273 (26)	0.092	1.6
0.5 *M*	1	80	0.307	26.7
	2	46 (3)	0.223	
		221 (18)	0.105	1.7
0+0.5 *M*	1	90	0.294	36.8
	2	44 (2)	0.212	
		219 (11)	0.116	3.2
	2	12	0.177 [c]	
		129	0.223	14.4
	3	2 (21)	0.055	
		46 (5)	0.212	
		229 (15)	0.110	3.0
	3	1 (0.6)	0.078 [c]	
		46 (2.7)	0.213	
		229 (13.7)	0.109	3.1
	3	2	0.085 [c]	
		⟨51⟩ [d]	0.220	
		⟨254⟩	0.095	3.2

[a] Number of exponential components.

[b] Uncertainties in θ from the diagonal elements of the covariance matrix.

[c] In this analysis r_0 was kept constant at value of 0.4. In all other analyses r_0 was a variable parameter.

[d] ⟨ ⟩ indicates fixed parameter in analyses.

parameters, i.e., two floating parameters (r_0 and θ_j) in the one correlation time fit, and four floating parameters (r_{01}, r_{02}, θ_1 and θ_2) in the two correlation time fit. Standard deviations, estimated from the diagonal elements of the covariance matrix (Table 2) display an improvement in resolution obtained by using collisional quenching and global analysis. The uncertainties in the correlation times recovered from global analysis are 2.5-fold smaller than those obtained from the non-quenched samples. The two correlation times of 44 and 219 ps correspond to local dynamics of the tyrosine (segmental motion) and overall rotational diffusion of the peptide.

It is of interest to consider the value of the initial anisotropy (r_0). More specifically, we now attempt to compare the apparent initial anisotropy recovered from the experimental data ($r(0) = \Sigma r_0 g_j$) with that found in vitrified solution in the absence of rotational diffusion (r_0). The anisotropy spectrum for enkephalin is shown as an insert in Fig. 2. In propylene glycol at −60°C there should be little if any tyrosyl motions during the excited state lifetime. At the experimental excitation wavelength of 287 nm we found $r_0 = 0.326$, which is in good agreement with the value recovered from the two correlation time analysis.

The value of r_0 observed at low temperature increases to slightly above 0.33 at the longest excitation wavelength. These values are considerably below the theoretical limit of 0.4 for colinear absorption and emission oscillators. The lower experimental initial anisotropy values can be a result of torsional oscillations occurring in solid and/or fluid media [33,34], or might be a result of an angular displacement between the orientations of the absorption and emission transition moments [35,36].

In recent reports time-zero anisotropies as high as 0.4 have been reported for tryptophan [37] and the single tryptophan protein melittin [38]. The case of indole or tryptophan is different due to the known presence of multiple transitions. In the case of tyrosine only a single electronic transition is thought to be present in the longest wavelength absorption band, and hence one may expect $r_0 = 0.4$. Hence we questioned whether our

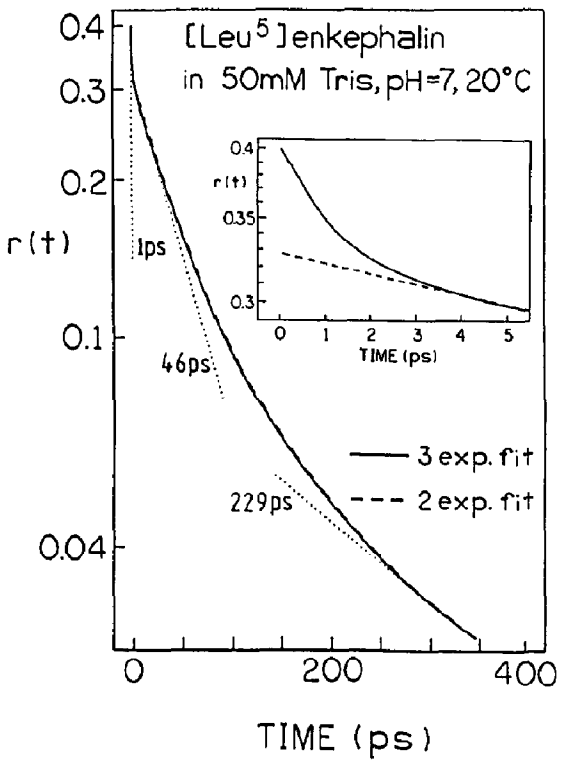

Fig. 3. Reconstructed anisotropy decay using decay parameters obtained from the frequency-domain data. The insert shows the initial loss of anisotropy in the first five picoseconds.

experimental data are consistent with an initial anisotropy of 0.4. To accomplish this we analyzed the data with the total anisotropy held fixed at 0.4. With this constraint, it was not possible to fit the data with two correlation times ($\chi^2_R = 14.4$). However, an acceptable fit was obtained with $r_0 = 0.4$ and three correlation times (Table 2). Surprisingly, the three correlation times show only modest standard deviations, suggesting they are well determined by the data. If r_0 is allowed to be a variable, then we could also recover three correlation times, but with unacceptable standard deviations (±21 ps for the shortest correlation time). Hence, the data are consistent with an initial 1–2 ps anisotropy decay with an amplitude of 0.075.

We used the three correlation time analysis with $r_0 = 0.4$ to construct the time-dependent anisotropy decay (Fig. 3). The initial 1.1 ps anisotropy decay time contributes during the ini-

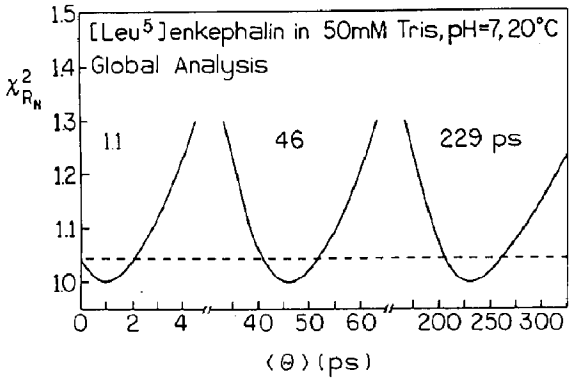

Fig. 4. Dependence of the goodness-of-fit parameter χ_R^2 on the correlation times of [Leu^5] enkephalin. In this three exponential anisotropy decay analysis the value of the fundamental anisotropy was fixed at 0.4 and all other parameters were floating.

tial 2 ps of the decay, after which the two and three correlation time fits yield equivalent anisotropy decays. It should be emphasized that one can see the presence of this initial component in the frequency-domain data. The 1.1 ps component results in somewhat larger phase angles (—) from 4 to 9 GHz (Fig. 2). The two correlation time model in Fig. 2 (---) does not account for the phase data at these frequencies. Also, these results illustrate the value of measuring anisotropy decay in the presence of collisional quenching, as the 1.1 ps motions are only evident in the frequency-domain data above 3 GHz (Fig. 2).

Assuming for the moment that one accepts the premise that $r_0 = 0.4$, it is then of interest to know the range of correlation times consistent with the data. These ranges were found from the χ_R^2 surfaces for the correlation times (Fig. 4). To construct these surfaces, we held one correlation time fixed at the value on the x-axis, and r_0 fixed at 0.4. Then, a least squares fit was performed to minimize χ_R^2. The range of values consistent with the data was taken as the values at which χ_R^2 was elevated so that there was only 33% chance that the increase was due to random errors in the data (the dashed line in Fig. 4). Based on these surfaces there is relatively little uncertainty in the correlation times, 1 ± 1 ps, 46 ± 5 ps and 229 ± 25 ps. We note that changing one of the correlation times to a slightly different value within the uncertainty limits does not result in much change in the other correlation times or amplitudes. This is illustrated in Table 2 where the two longer correlation times were held fixed at the upper uncertainty limit. In this case the amplitudes are similar, and the 1.1 ps component remains at 2 ps or smaller.

4. Discussion

Frequency-domain data to 10 GHz provide picosecond resolution of multiexponential tyrosyl intensity and anisotropy decays of [leu^5] enkephalin. The resolution was further enhanced by the use of collisional quenching, followed by global analysis of the data from the quenched and unquenched samples. These highly resolved anisotropy decays are on a timescale which allows comparison with molecular dynamics simulations on this peptide.

Our frequency domain data are consistent with an initial loss of 20% of the total anisotropy on a timescale of about 1 ps. However, detection of this component requires the assumption that the initial anisotropy at $t = 0$ is 0.4. This initial loss, if present, could be due to torsional oscillations on the ps timescale. Theoretical studies of the molecular dynamics of proteins [7] have demonstrated that significant atomic fluctuations occur in the protein interior on the picosecond time scale. The fluorescence depolarization depends on the decay of the angular correlation functions and the initial rate of the anisotropy decay reflects the rate of the fast peptide motions. Levy and Szabo [39] used molecular dynamics simulations to calculate initial fluorescence depolarization of tyrosine in proteins, and found that $r(t)$ decays to a plateau value in about 2 ps, as has been suggested by Nordlund and co-workers for tyrosine residues in proteins [40]. Alternatively, Hochstrasser and co-workers have detected r_0 values less than 0.4 for aniline and suggested vibronic coupling to the electronic state as causing the rapid loss of polarization [41]. If the resolution of the fluorescence depolarization experiment is less than 2 ps, then $r(t)$ decays with a correlation time corresponding to the slower seg-

mental and overall motions of the protein. Ichize and Karplus [42] also used molecular dynamics to calculate the anisotropy decays of a protein, in this case lysozyme. They found that initial depolarizations occur within 0.5 to 5 ps, depending upon the location of the tryptophan residue. The present data do not allow an unambiguous assignment of the mechanism causing the initial loss of anisotropy. However, we believe that our 10 GHz frequency-domain fluorometer can provide data adequate to recover the initial portion of the anisotropy decays of tyrosine or tryptophan fluorescence from proteins, and that the time resolution is adequate for comparison with molecular dynamics calculations.

Acknowledgements

This work was supported by grant DMB-8804931 from the National Science Foundation, with support for instrumentation from NSF grant D1R-8710401, and NIH grant S10 RR07510. Joseph R. Lakowicz, Gabor Laczko and Wieslaw Wiczk acknowledge support from the Medical Biotechnology Center at the University of Maryland School of Medicine.

References

1 J.R. Lakowicz (ed.), Time-resolved laser spectroscopy in biochemistry II, Proc. SPIE 1640 (SPIE, Bellingham, WA, 1992).
2 A.P. Demchenko, Ultraviolet spectroscopy of proteins (Springer Verlag, New York, 1987).
3 S.T. Ferreira, Biochemistry 28 (1989) 10066–10072.
4 T.M. Nordlund, X.Y. Liu and J.H. Sommer, Proc. Natl. Acad. Sci. USA 83 (1986) 8977–8981.
5 R.F. Steiner, Topics in fluorescence spectroscopy, Vol. 2: Principles, ed. J.R. Lakowicz (Plenum Press, New York, 1991) pp. 1–52.
6 J.A. McCammon and S.L. Harvey, Dynamics of proteins and nucleic acids, (Cambridge University Press, New York, 1987).
7 M. Karplus and J.A. McCammon, CRC Crit. Rev. Biochem. 9 (1981) 293–349.
8 M. Karplus, Meth. Enzymol. 131 (1986) 283–307.
9 A.J.W.G. Visser (ed.), Anal. Chem. 14 (1985) 193–566.
10 D.V. O'Connor and D. Phillips, Time-correlated single photon counting (Academic Press, New York, 1984).
11 J.R. Lakowicz, G. Laczko and I. Gryczynski, Rev. Sci. Instrum. 57 (1986)2499–2506.
12 G. Laczko, I. Gryczynski, Z. Gryczynski, W. Wiczk, H. Malak and J.R. Lakowicz, Rev. Sci. Instrum. 61 (1990) 2331–2337.
13 E. Gratton and M. Limkeman, Biophys. J. 44 (1983) 315–324.
14 J.R. Lakowicz, E. Gratton, G. Laczko, H. Cherek and M. Limkeman, Biophys. J. 46 (1984) 463–477.
15 E. Gratton, M. Limkeman, J. Lakowicz, B. Maliwal, H. Cherek and G. Laczko, Biophys. J. 46 (1984) 479–486.
16 J.R. Lakowicz, H. Cherek, B. Maliwal and E. Gratton, Biochem. 24 (1985) 376–383.
17 J.R. Lakowicz, G. Laczko, I. Gryczynski and H. Cherek, J. Biol. Chem. 261 (1986) 2240–2245.
18 J.R. Lakowicz, G. Laczko and I. Gryczynski, Biochem. 26 (1987) 82–90.
19 J.R. Lakowicz, M.L. Johnson, N. Joshi, G. Laczko and I. Gryczynski, Chem. Phys. Lett. 131 (1986) 343–348.
20 J.R. Lakowicz, H. Szmacinski and I. Gryczynski, Photochem. Photobiol. 47 (1988) 31–41.
21 Lakowicz, J.R. and B. Maliwal, J. Biol. Chem. 258 (1983) 4794–4801.
22 W.R. Laws, J.B.A. Ross, H.R. Wyssbrod, J.M. Beechem, L. Brand and J.C. Sutherland, Biochem. 25 (1986) 599–607.
23 J.B.A. Ross, W.R. Laws, A. Buku, J.C. Sutherland and H.R. Wyssbrod, Biochem. 25 (1986) 607–612.
24 T.L. Nemzek and W.R. Ware, J. Chem. Phys. 62 (1975) 477–489.
25 J.R. Lakowicz, M.L. Johnson, N. Joshi, I. Gryczynski and H. Cherek, J. Phys. Chem. 91 (1987) 3277–3285.
26 J.R. Lakowicz, N.B. Joshi, M.L. Johnson, H. Szmacinski and I. Gryczynski, J. Biol. Chem. 262 (1987) 10907–10910.
27 Lakowicz, J.R. and B. Maliwal, J. Biol. Chem. 258 (1983) 4794–4801.
28 J.R. Lakowicz, H. Cherek, I. Gryczynski, N. Joshi and M.L. Johnson, Biophys. J. 51 (1987) 755–768.
29 I. Gryczynski, H. Cherek and J.R. Lakowicz, Biophys. Chem. 30 (1988) 271–277.
30 Maliwal, B.P. and J.R. Lakowicz, Biochem. Biophys. Acta 873 (1986) 173–181.
31 J.R. Lakowicz, B. Maliwal, H. Cherek and A. Balter, Biochemistry 22 (1983) 1741–1752.
32 Lakowicz, J.R. and B. Maliwal, J. Biol. Chem. 258 (1983) 4794–4801.
33 J. Perrin, 2^{me} Conseil de Chim. Solvay (Gauthier-Villars, Paris, 1925) p. 322.
34 A. Jablonski, Acta Phys. Polon. 28 (1965) 717–722.
35 G. Weber, in: Fluorescence and phosphorescence analysis, ed. D.M. Hercules (Wiley, New York, 1966) pp. 217–240.
36 S.V. Konev, Fluorescence and phosphorescence of protein and nucleic acids (Plenum Press, New York, 1967).
37 J.E. Hansen, S.J. Rosenthal and G.R. Fleming, J. Phys. Chem. 96 (1992) 3034–3040.

38 A.J. Ruggiero, D.C. Todd and G.R. Fleming, J. Am. Chem. Soc. 112 (1990) 1003–1014.
39 R.M. Levy and A. Szabo, J. Am. Chem. Soc. 104 (1982) 2073–2075.
40 X.Y. Liu and T.M. Nordlund, Proc. SPIE 1204 (SPIE, Bellingham, WA, 1990) pp. 669–675.
41 A.B. Myers, M.A. Pereira, P.L. Holt and R.M. Hochstrasser, J. Chem. Phys. 86 (1987) 5146–5155.
42 T. Ichize and M. Karplus, Biochemistry 22 (1983) 2884–2893.